Identification of novel genes involved in phosphate accumulation in *Lotus japonicus* through Genome Wide Association mapping of root system architecture and anion content

Marco Giovannetti[1*], Christian Göschl[1], Stig U. Andersen[2], Stanislav Kopriva[3], Wolfgang Busch[1,4*]

[1]Gregor Mendel Institute (GMI), Austrian Academy of Sciences, Vienna Biocenter (VBC), Vienna, 1030 Austria; [2]Department of Molecular Biology and Genetics, Aarhus University, 8000 Aarhus C, Denmark; [3]University of Cologne, Botanical Institute and Cluster of Excellence on Plant Sciences (CEPLAS), D-50674 Cologne, Germany; [4]Salk Institute for Biological Studies, Plant Molecular and Cellular Biology Laboratory, and Integrative Biology Laboratory, La Jolla, CA, 92037 USA

*Corresponding Authors: Marco Giovannetti (marco.giovannetti@gmi.oeaw.ac.at)
Wolfgang Busch (wbusch@salk.edu)

Running title: GWAS on Lotus japonicus root system architecture and anions

Abstract

Phosphate is a key nutrient for plants and as it is needed in high quantities. It is highly immobile in the soil and represents a major limiting factor for plant productivity. Plants have evolved different solutions to forage the soil for phosphate and to adapt to phosphate limitation ranging from a profound tuning of their root system architecture and metabolic profile to the evolution of widespread mutualistic interactions, such as those with arbuscular mycorrhizal fungi (AM symbiosis). Despite the prevalence of AM symbiosis throughout land plants, most studies aimed at identifying genes that regulate plant responses to phosphate have been conducted in species incapable of AM symbiosis, such as Arabidopsis. Here we elucidated plant responses and their genetic basis to different phosphate levels in a plant species that is widely used as a model for AM symbiosis: *Lotus japonicus*. Rather than focusing on a single model strain, we measured root growth and anion content in response to different levels of phosphate in a large panel of Lotus japonicus natural accessions. This allowed us not only to uncover common as well as divergent responses within this species, but also enabled Genome Wide Association Studies by which we identified new genes regulating phosphate homeostasis in Lotus. Under low phosphate conditions, we uncovered a correlation between plant biomass and the decrease of plant phosphate concentration in plant tissues, suggesting a dilution effect. Altogether our data of the genetic and phenotypic variation within a species capable of AM complements studies that have been conducted in Arabidopsis, and advances our understanding of the continuum of genotype by phosphate level interaction that exists throughout dicot plants.

Author Summary

Phosphate represents a major limiting factor for plant productivity. Plants have evolved different solutions to adapt to phosphate limitation ranging from a profound tuning of their root system architecture and metabolic profile to the evolution of widespread mutualistic interactions, such as arbuscular mycorrhizal symbiosis. Here we elucidated plant responses and their genetic basis to different phosphate levels in model legume plant species, *Lotus japonicus*, a plant commonly used for studying arbuscular mycorhizal symbiosis. We investigated Lotus responses to phosphate levels by combining high throughput root system architecture phenotyping and nutrient measurements with a natural variation approach. We investigated relations between root phenotypic responses and nutrient accumulation and we uncovered, under low phosphate conditions, a correlation between plant biomass and the decrease of plant phosphate concentration in plant tissues, suggesting a dilution effect. By means of Genome Wide Association mapping and integration of multiple traits, we identified new genes regulating phosphate homeostasis in Lotus.

Introduction

Phosphate is an essential element for plant growth and its bioavailability represents a major limiting factor for plant productivity. Plants coping with phosphate deficiency exhibit dramatic changes at the developmental, nutritional and metabolic levels. For example, in *Arabidopsis thaliana,* the root developmental program has been described to be highly affected by phosphate deficiency. Primary root growth of the reference accession Col-0 is inhibited and there is an

69 increase of lateral root formation and root hair growth (López-Bucio et al., 2002). The key
70 genetic determinants of this process have been identified, mainly through forward genetic
71 screening (Svistoonoff et al., 2007; Wang et al., 2019). Recently, it has been shown that a main
72 driver of primary root growth arrest is toxicity of iron that, upon phosphate starvation,
73 accumulates in the meristematic zone and induces a progressive loss in the proliferative capacity
74 of the cells, causing reduction in meristem length (Müller et al., 2015). Plants facing phosphate
75 starvation exhibit a dramatic remodeling of main cellular processes: a transient DNA methylation
76 altering gene transcription (Secco et al., 2015), mainly driven by the phosphate-dependent
77 interaction of SPX1/PHR1 (Puga et al., 2014). In addition, phosphate-depleted plants usually
78 display a high turnover of phospholipids into sulfolipids (Essigmann et al., 1998). Furthermore,
79 there is a substantial interaction of phosphate related processes and other environmental factors.
80 For instance, red light frequencies lead to an increase of phosphate uptake and Arabidopsis
81 accessions with light-sensing defects, such as Lm-2 and CSHL-5, take up less phosphate
82 (Sakuraba et al., 2018). Moreover, phosphate accumulation is altered by the abundance of metal
83 ions, such as iron and zinc, with the extent of the impact being dependent on the genetic
84 background (Briat et al., 2015; Kisko et al., 2018). Taken together, responses to phosphate and
85 phosphate homeostasis in plants are regulated in a complex manner and are substantially
86 dependent on plant genetic diversity and environmental abiotic and biotic factors.
87 For biotic factors, it was recently shown in Arabidopsis and related plants how fungi and bacteria
88 play a key role in mediating phosphate accumulation (Almario et al., 2017; Hiruma et al., 2016).
89 Molecular hubs of phosphate metabolism, such as PHR1, can define the composition of
90 microbial communities (Castrillo et al., 2017) and the analysis of microbial contribution to plant
91 phosphate accumulation can even be mathematically modeled, giving rise to the possibility to

92 design ad-hoc microbial communities with desired effects on plant phosphate uptake (Paredes et
93 al., 2018). The most prominent example of microorganisms providing plants with phosphate is
94 the symbiosis of plants with arbuscular mycorrhizal (AM) fungi. A key aspect of this is that
95 fungal hyphae are very efficient in exploring the soil and taking up the highly immobile
96 phosphate. Consequently, up to 80% of the needed phosphate can be acquired and transferred to
97 plants by these fungi (for up-to-date reviews Choi et al., 2018; Lanfranco et al., 2018; MacLean
98 et al., 2017). Numerous plant genetic determinants that are needed for the establishment of a
99 functional mycorrhizal symbiosis have been described over the last 20 years but a lack of high-
100 throughput methods and the complexity of the system impaired the comprehensive
101 understanding of the crucial and complex feedback happening between plant phosphate status
102 and the establishment of AM symbiosis (Carbonnel and Gutjahr, 2014).
103 Most genetic screens aiming for identifying genes that regulate plant responses to phosphate
104 have been conducted in species incapable of AM symbiosis such as Arabidopsis. In this study we
105 targeted the genetic basis of responses to phosphate levels in a plant widely used as a model for
106 AM symbiosis. To do so, we conducted large-scale studies of *Lotus japonicus* natural variation
107 of root responses to different levels of phosphate, coupled with the measurements of anion
108 accumulation. We discovered profound correlations of plant size and plant phosphate
109 concentration that should be taken into account when working with concentration measures.
110 Using high-density SNP data from the 130 Lotus accessions, we conducted Genome Wide
111 Association Studies (GWAS) for all measured traits, finding hundreds of genetic loci associated
112 with variation in phosphate-related traits. Finally, by comparing the lists of candidate genes for
113 root system architecture and phosphate accumulation, we identified a Leucine-Rich Receptor
114 kinase and a cytochrome B5 reductase involved in phosphate homeostasis as high confidence

115 causal genes, which was further corroborated by phosphate dependent phenotypes of loss of
116 function mutants for these genes.
117
118 **RESULTS**
119 **Phosphate deficiency shapes natural variation of root growth and anion levels in roots and**
120 **shoots of *Lotus japonicus***
121 To study the genetic bases of root responses to low phosphate and phosphate accumulation in
122 *Lotus japonicus* (Lotus) tissues, we performed a detailed root phenotyping of a panel of 130
123 diverse Lotus natural accessions (Shah et al., 2018) over a 9-day time course and subsequently
124 quantified the anions of the main macronutrients from the same material (Fig. 1a). In particular,
125 we grew the plants on vertical plates for 9 days on a modified Long-Ashton medium
126 (Supplemental Table 1), containing either 20 µM (LP) or 750 µM (HP) of phosphate. We
127 scanned the plates daily, at the same time of the day and at the end of the 9th day, we harvested
128 and weighed total root and total shoot (stem and leaves) material for subsequent quantification of
129 main macronutrients: nitrate, phosphate and sulfate.
130 As shown in Figure 1b-c, wide variation among macronutrient concentrations is observed in
131 different accessions. Phosphate levels in the medium not only affect plant phosphate
132 concentration in roots and shoots, but also plant sulfate levels and, to a minor extent, nitrate
133 concentration in roots, exposing a similar cross-talk between the three anions in Lotus as the one
134 that had been described in Arabidopsis (Kellermeier et al., 2014). With the exception of
135 phosphate concentration of plants grown under phosphate starvation, the concentration of these
136 anions did neither depend on plant size nor on plant developmental stage (Supplemental figure
137 1).

By using a modified version of the Brat Fiji plugin (Giovannetti et al., 2017; Slovak et al., 2014), we quantified 16 root traits per each day. Root traits showed a broad spectrum of responses among accessions (Fig. 1d,e). There was a pronounced effect of phosphate on the majority of traits and interactions of effects between genotype and phosphate (Supplemental file 1). We then explored whether the response to phosphate levels merely reflects the genetic relation between Lotus natural accessions. For this we conducted hierarchical clustering of root growth and root tip width in both phosphate levels and found that the clusters do not reflect the established genetic Lotus subpopulation structure (Shah et al., 2018) but rather depend on phosphate level in the medium (Fig. 1d,e). In contrast to the early root growth responses described in the Arabidopsis reference accession, low phosphate medium does not induce a dramatic arrest of primary root growth in most of the Lotus accessions (Supplementary Fig. 2a). Similar PR responses have also been also observed in non-reference Arabidopsis accessions (Chevalier et al., 2003), the diversity of root growth responses to phosphate levels in Lotus seems to resemble that in Arabidopsis. Beyond total root length, root traits related to the root diameter, such as root width, are substantially influenced by phosphate deficiency: the width of the first 20% adjacent to the root/shoot junction (denominated as trait "Root width 20") and the distal 20% ("Root width 100"), do get larger over time in plants grown in HP (Suppl. Fig. 2 b,c).

The broad sense heritability (BSH) was different among the traits that we measured. While the variation of some traits could not be explained by genetics (Root linearity and root angle, ~0%), most traits are genetically determined and some to an extraordinarily high degree (root_SO4, 86%). Generally, traits related to nutrient accumulation showed higher heritability (Fig. 2a). Among the root developmental traits, total root length showed the highest BSH (~60%), consistently with data from other root system architecture studies in *Arabidopsis thaliana*

(Ristova et al., 2018).

Taken together, we found that Lotus natural accessions exhibit a great variation of responses to phosphate concentrations, both at the phenotypic and at metabolic level. Moreover, the similar profound extent of natural variation of root growth between Arabidopsis and Lotus suggests that a large genotype by phosphate level interaction exist within species throughout the dicot group and regardless of whether a species is capable to form AM symbiosis.

There is a trade-off of root phosphate concentration and root length specifically under low phosphate conditions

Phosphate starvation has a profound impact on root development and nutrient accumulation. Nevertheless, the link of the two processes remains largely unknown . Since we quantified phosphate, sulfate and nitrate concentrations from roots and shoots of single plants, and also measured root traits over time, we were able to compare trait correlations in LP or HP. This represents a valuable dataset to investigate the links between plant developmental adaptations and cellular metabolic tuning. For this, we calculated the pairwise Pearson's correlation coefficients of all root trait data and anion content in high and low phosphate from all Lotus accessions (Fig. 2b). The contrasting phosphate levels in the two media did not perturb the majority of correlations among traits (Fig. 2b): for example root width at different sectors along the root were highly positively correlated regardless of phosphate level, as well as the traits related to root length (Euclidian length, root growth rate, total length and relative root growth rate). Root length was negatively correlated with root width, in both conditions, indicating that longer roots are usually thinner in our working conditions.

Nevertheless, we could observe several peculiar correlations occurring exclusively in one of the

two conditions: first, the ratio of phosphate concentration between shoot and root, that describes how much of the uptaken phosphate is transferred to the shoot, is significantly negatively correlated with root length and positively correlated with root width under HP but not LP (Fig. 2c). This indicates that under HP less phosphate is allocated to the shoot when roots are elongating. However, when phosphate becomes limiting in the medium (LP), the total length of roots and root phosphate concentration are moderately negatively correlated (Fig. 2b and supplementary fig. 3). This suggests a model in which under LP the available phosphate is distributed over a larger amount of root tissue if roots are longer and is thereby diluted. This dilution model would furthermore also explain the negative correlation between plant biomass and phosphate concentration (Suppl figure 1). By contrast, and in agreement with this dilution model, the negative correlation of phosphate levels and root length is completely absent in HP media (Fig 2c) and much reduced when considering plant biomass and phosphate concentration (Suppl figure 3).

Altogether a parallel quantification of phosphate accumulation and root system architecture of a panel of 130 Lotus grown at two different phosphate concentrations allowed for the detection of trait correlation structure, showing that most of trait-correlation are not perturbed by phosphate levels. Our analysis also revealed that, in our experiment, the majority of nutrient accumulation traits show higher broad sense heritability compared to root developmental traits.

GWAS for Lotus phosphate related traits identifies hundreds of unknown and known candidate genes for phosphate homeostasis

Given the extensive natural variation of most traits in the Lotus panel, we conducted a Genome Wide Association Study (GWAS) for each trait and each time point in LP and HP condition,

using a mixed model algorithm, corrected for population structure (Yu et al., 2006; Kang et al., 2008; Seren et al., 2012) and using sequencing-based SNPs for the Lotus accessions (Shah et al., 2018). Each trait led to the identification of genetic loci significantly associated with variation of those traits: using a Benjamini-Hochberg FDR threshold of 5%, we found 900 SNPs associated with root growth parameters of plants grown on LP media (Supplementary table 3), 939 SNPs with HP conditions (Supplementary table 4), 3673 of LP/HP root growth ratio (Supplementary table 2), 104 associated with phosphate content and 220 with anion content (Supplementary table 5 and 13).

Several obvious candidate genes were in these lists. For genes associated with morphological root traits, our analysis identified homologues of several known regulators of root development, such as an homologous gene of SCARECROW (Di Laurenzio et al., 1996), Lj3g3v0821320, associated with Root horizontal index at day 6 under low phosphate conditions. Similarly, sequence variation in the genomic region of a Lotus BIG BROTHER homologue (Cattaneo and Hardtke, 2017), Lj3g3v0489450, is associated with relative root growth rate over day 1-2. Another candidate gene identified as a potential regulator of Lotus root responses to low phosphate is the homologous gene of STOP1 (Lj0g3v0231229) that is associated with Root width 20 variation at day 3. In Arabidopsis, STOP1 was recently described as a key regulator of early root responses to phosphate deficiency-induced iron toxicity (Mora-Macías et al., 2017; Balzergue et al., 2017), therefore a similar role is conceivable for Lotus. Various fatty acyl-CoA reductases are highly associated with root width 80 day 2 and have been shown to be involved in alcohol synthesis as response to various stress and suberin accumulation (Domergue et al., 2010). In parallel, the quantification of phosphate concentration at root and shoot level for the Lotus natural accessions grown at two different levels of phosphate led to the identification of several

genetic loci associated with variations in those traits. Among the genes associated with phosphate concentration-related traits, we identified a trehalose-phosphate phosphatase-like protein (Lj4g3v2820240) associated with $shoot_{[PO4]}$:$root_{[PO4]}$ in LP. A significant association was also detected for a SNP within a UDP-glucuronic acid decarboxylase gene (Lj4g3v2312430), associated with shoot phosphate concentration in HP plants. Variation in the genetic region spanning a candidate sugar/phosphate translocator (Lj1g3v4830440) is correlated with root phosphate concentration in HP, as well as a UDP pyrophosphate phosphatase (Lj0g3v0276539) associated with shoot phosphate concentration in HP. Altogether many genes related to phosphate recycling seem to be linked with phosphate accumulation in shoots and roots in both media conditions, even though GO enrichment analysis does not highlight any obvious category (Suppl. Table 11 and 12).

Overlap among Lotus GWAS from different traits exposes loci associated with both Lotus root growth upon phosphate starvation and phosphate accumulation

Beyond investigating specific genetic associations between Lotus SNPs and particular root traits or phosphate accumulation values, one of our main interests within this study was to use both our metabolic and root growth data to specifically determine genes that control Lotus responses to phosphate. To accomplish that, we considered all genes in 10 kb genomic regions (Linkage Disequilibrium decays in Lotus, $r^2<0.2$, with 10 kb (Shah et al., 2018)) centered on the SNPs passing our GWAS detection threshold. Because it was our purpose to assess overlaps, we took a non-conservative threshold for this approach. We considered up to 500 SNPs with a Benjamini-Hochberg threshold of 10^{-5} for the two groups of traits: phosphate content and root system architecture. This approach led to an overlap consisting of only 7 genomic regions (Supplemental

table 8) that were associated with both root and phosphate accumulation traits. These regions were in close proximity to 13 genes (Fig. 3a). We focused on two of these regions, each encompassing a single protein coding gene that was expressed in roots (according to publicly available expression data (Mun et al., 2016) and had possible functions related to signaling and/or acquisition of phosphate. One locus was associated with $shoot_{[PO4]}$:$root_{[PO4]}$ on HP and root tortuosity at day 2 on LP (Fig. 3b and supplementary figures 8 and 9) and the other locus was associated with root phosphate concentration on LP and root width 80 at day 1 on LP (Fig. 3c). Interestingly, this locus was also associated with LP:HP root growth rate between day 7 and day 8 (Suppl. table 2). To further validate an existing interaction among these two pairs of traits, we also performed a multitrait GWAS, based on LIMIX (Casale et al., 2015; Turley et al., 2018), a mixed-model approach enabling analysis across multiple traits while accounting for population structure. Consistently with our overlap analysis, the same loci are associated with both traits for which they were detected (Suppl. Fig 10 and 11), therefore constituting suitable candidate genetic regions associated with Lotus root responses to phosphate.

In both cases, the above mentioned SNPs span a 10kb LD region with exclusively one protein-coding gene that is expressed in roots: Lj0g3v0008839, coding for a LRR receptor-like serine/-rich (LRR-RK) protein on chromosome 0 and Lj3g3v3688850, a putative cytochrome b5 reductase (CYT). To test whether these candidate genes have a role in controlling responses to phosphate level, we selected multiple insertional mutants for each gene from Lotus Base (Małolepszy et al., 2016; Mun et al., 2016) as represented in Fig. 4a. We quantified the tissue phosphate concentration in homozygous mutant plants for both genes in three different phosphate concentrations (20, 100 and 750 μM), 10 days after transfer to specific media plates (Figure 4b,c). All three independent mutant lines of the LRR-RK showed an increased total plant

phosphate concentration on high phosphate concentrations (Figure 4b,c and Supplementary table 7). Accordingly, we named the gene *LAMP* (**L**RR-RK **A**ccumulating **M**ore **P**hosphate). Two out of three CYT mutant lines showed an increased total plant phosphate concentration on high phosphate concentrations, specifically driven by shoot phosphate levels (Supplementary figure 5). The WT-like responding mutant line was different in the transposon insertion site with respect to the other two mutant lines and still might have some remaining activity of the protein due to transposon insertion at the far end of the gene (Fig. 4a). While the observable effects of the loss of function of these two genes was significant in HP, a diverse and variable phosphate accumulation took place in LP conditions. We reasoned that the effect of LP on biomass and root length that we had observed earlier (Suppl. Fig. 1) might confound the effects on phosphate content. Therefore we assessed these correlations also across the wt and LORE1 insertion lines. As found within the large panel of accessions, we observed that total phosphate concentration from mutant and wt plants grown under strong or mild phosphate starvation (20, and 100 μM) was strongly negatively correlated with plant biomass (ρ=-0.58, ρ=-0.55, respectively) (Fig. 5), but this correlation is completely absent under HP (750 μM). Interestingly the stronger correlations are more pronounced considering the whole plant compared to root or shoot separately (Suppl. Fig. 6). While we selected these two candidate genes for being associated with phosphate level dependent phosphate content as well as root growth traits, we could not observe a consistent and significant root growth difference to wildtype in any of the tested phosphate concentration (Suppl. Fig 7).

Altogether, we provided the community with an atlas of root growth and anion related Lotus phenotypes, showed that root system variation within a genotype by phosphate interaction is not specific to Arabidopsis but also happens in a plant able to form AM symbiosis -even in the

299 absence of the symbiont-, we generated a catalogue dataset of genes associated with root and
300 metabolite responses to phosphate, we investigated phenes and cross-links shaping Lotus natural
301 variations of responses to phosphate and we genetically validated new candidate genes involved
302 in phosphate accumulation. Lastly, a clear confounding element has been unveiled that could
303 prevent future inappropriate conclusions.
304
305 **Discussion**
306 In this study, we generated a comprehensive atlas of root system architecture and nutrient
307 accumulation responses to two levels of phosphate in 130 accessions of *Lotus japonicus* and
308 studied trait relationships, their genetic basis and identified two genes controlling accumulation
309 of phosphate. Overall, our results exposed general patterns of phenotypic and metabolic
310 responses to phosphate, as well as significant natural variation in these responses across Lotus
311 accessions, which importantly were not necessarily related to the Lotus subpopulation classes
312 (Fig. 1d,e). This indicates that population structure doesn't confound to a large extent when
313 studying responses to phosphate levels and don't preclude screening for natural allelic variants
314 that underlie these traits.
315
316 **Root responses to phosphate and the heritability of root and anion content traits**
317 Low phosphate has been mostly associated with the inhibition of primary root growth and this
318 process has been shown to be regulated by phosphate dependent iron toxicity in the Col-0
319 Arabidopsis reference accession. However, it is not frequently considered that other Arabidopsis
320 accessions are not showing any inhibition of primary root growth upon phosphate starvation
321 (Chevalier et al., 2003), a finding that had indicated that this response is not canonical. In line

with that, phosphate deficiency dependent inhibition of early root growth was not observed in our Lotus panel as LP does only have a minor effect on Lotus primary root growth (Suppl fig. 2). This is consistent with previous reports for Lotus MG-20 ecotype (Volpe et al., 2016). Our data shows a broad variation of root growth responses among Lotus accessions, depending on phosphate availability. Altogether this points towards different adaptive strategies that have been selected in the Lotus natural populations in order to cope with phosphate starvation in their natural soil environments, in a similar manner to the natural variation of this response that has been described in Arabidopsis natural accessions.

Hierarchical clustering among accessions does depend on the phosphate level and not on the Lotus subpopulation (Fig. 1d-e), indicating that the observed responses to phosphate are not just an expression of the kinship of these accessions.

Beyond highly heritable traits, such as flowering time (Atwell et al., 2010) and seed dormancy (Kerdaffrec et al., 2016), whose variation strongly depends on plant adaptation to environmental conditions, in the last years different studies successfully used GWA for identifying genes and alleles regulating both plant nutrient concentration and root growth traits. By measuring plant cadmium (Chao et al., 2014), sulfur (Koprivova et al., 2013; Huang et al., 2016), sodium (Baxter et al., 2010) and phosphate (Kisko et al., 2018) tissue concentration, causal genes were identified. A similar approach has been used to trace and map root growth responses to iron deprivation (Satbhai et al., 2017), salt stress (Julkowska et al., 2017), zinc (Bouain et al., 2018), nitrogen (Gifford et al., 2013) and phosphate (Stetter et al., 2015) levels. In our attempts to integrate the two last approaches and recapitulate the natural variation of Lotus phosphate accumulation and root system architecture responses to phosphate levels, we observed a great variability among broad sense heritability between the two groups of traits (Fig. 2a).

345 Interestingly, in our set up, the majority of traits related to anions showed higher BSH compared
346 to root growth related traits, with the exception of primary root growth length. Lower BSH
347 reflects a higher trait variance within genotype compared to the trait variance found across
348 genotypes. We therefore expect that traits showing higher BSH are either highly responsive to
349 the external environmental conditions and factors not taken into account in our experimental set-
350 up, such as plate micropatterning or seed size, or that our measurement error was too high for
351 those traits. Another possible reason for the difference of BSH between these trait classes could
352 be the different number of replicates: for the RSA analysis, we analysed 8 biological replicates,
353 whereas the anion content was based on 4 biological replicates. Nevertheless, the higher BSH did
354 not result in larger number of significantly associated SNPs for single anion traits
355 (Supplementary figure 4).

356 **Relation of phosphate content and root growth**

357 During our investigation we found a surprising correlation between phosphate content and
358 growth related traits exclusively in LP conditions (Fig. 2c): the longer the root, the less
359 concentrated the phosphate. The most likely explanation for this seems to be that we observe
360 phosphate dilution effect in which the limited amount of P that is available in the plant is
361 distributed over a larger amount of tissue in case of larger accessions. Our initial observation on
362 a broad panel of accessions, became even more evident when focusing on a single genetic
363 background (Gifu), where less genetic confounding effect are present (Fig. 5). In this scenario,
364 when plants are grown under low (20 μM) and mid (100 μM) phosphate, an even stronger and
365 more significant negative correlation between plant biomass and plant phosphate concentration
366 emerges. Again, this correlation is completely absent from plant grown under sufficient
367 phosphate concentration (750 μM). It would not be surprising if a similar correlation could be

368 observed for other main limiting factors for plant growth, such as nitrogen, sulfur or potassium.
369 While it has been described in *Brassica oleracea* that shoot yield drives phosphorus use
370 efficiency and correlates with root architecture traits (Hammond et al., 2009), this process seems
371 not to have been described before. A possible reason this link was not previously described could
372 be that the whole-single-plant resolution is usually missing. In fact, in experiments performed in
373 Arabidopsis, many plants are usually bulked together before measuring any content and therefore
374 extreme values are lost, therefore possibly occluding correlations. Conversely, in studies
375 focusing on crop plants, due to the plant size, only a part of it is usually considered, therefore
376 possibly missing organismal correlations. Given that nutrient levels are also responsible of a
377 downstream cascade of gene transcription and cellular reprogramming (in the case of phosphate
378 starvation they depend on PHR1 transcription factor), we think that plant biomass should always
379 be taken into account when dealing with nutrient starvation condition, to avoid recursive
380 confounding effects.
381
382 **Candidate genes for phosphate homeostasis**
383 Phosphate is one of the main macronutrients and a limiting factor for plant growth, which is
384 highly variable in natural and agricultural soils (Orgiazzi et al., 2018). We therefore expect a
385 strong selection on plant genomes due to soil phosphate concentration and/or soil
386 microenvironment (both biotic and abiotic). Nevertheless only few studies have identified causal
387 genes involved in plant phosphate nutrition in the light of natural variation (for example Kisko et
388 al., 2018; Stetter et al., 2015; Yang et al., 2012). By contrast, much more detailed knowledge has
389 been acquired through forward genetics screening and transcriptomics approaches (mainly in
390 Arabidopsis and rice) and subsequent validation of candidate genes.

391 Our GWAS analysis has detected hundreds of significant associations, among which are known
392 regulators of plant root responses to low phosphate, such as *STOP1*. By combining candidate
393 genes that were overlapping among traits, an approach that was similarly used in cereals (Chen et
394 al., 2016), we selected and validated two of these, a Leucine-Rich-Repeat receptor kinase and a
395 cytochrome B5 reductase. For each of these candidate genes, multiple LORE1 insertional
396 mutants accumulate more soluble phosphate than the wt plants on high phosphate media (Fig. 4).
397 However, despite the candidate genes being also associated with root traits, the mutants did not
398 show aberrant root phenotypes. This could be due to various reasons: for instance, redundancy or
399 genetic buffering might compensate for these genes for early root growth, the same loci might
400 have a minor effect on RSA and stronger effect on phosphate levels and/or the same SNPs were
401 in LD with other genes that could control RSA.
402 Despite the lack of early root phenotype, the clear involvement of these genes in the control of
403 root phosphate concentration exposes two new phosphate regulating genes, which are among the
404 first phosphate regulators known in Lotus. The Arabidopsis homologue of the cytochrome B5
405 reductase, CBR1 (Oh et al., 2016), was recently described as a crucial factor for iron uptake due
406 to its role in activating plasma membrane H^+-ATPase, responsible for acidification of the
407 rhizosphere. CBR1 is involved in energy transfer at the ER level, it therefore could also control
408 other important plant ion pumps that depends on electron potential. The inactivation of the Lotus
409 homologue leads to the accumulation of phosphate in plant cells, even though the localization
410 and the pool partitioning remains to be uncovered. *LAMP*, the LRR-RK is involved in regulating
411 internal plant phosphate levels and might therefore, similarly to other plant membrane receptors
412 that regulate nitrogen metabolism in Arabidopsis and/or rhizobial abundance in Lotus (Tabata et
413 al., 2014; Okamoto et al., 2013), be involved in nutrient signalling.

414 We are aware that further functional studies are needed to mechanistically understand their role
415 in phosphate uptake and/or recycling, eventually taking into account potential ligands such as
416 regulatory peptides that are utilized for signalling during phosphate starvation.
417
418 **Material and methods**
419 **Plant material and growth conditions**
420 In total, 130 *Lotus japonicus* accessions were used (Shah et al., 2018). The names and accession
421 numbers are listed in Supplementary Table 6. Seeds were scarified with sandpaper and then
422 sterilized 14 minutes in 0.05% sodium hypochlorite. Subsequently, seeds were rinsed and
423 washed 5 times in sterile distilled water. For the germination, seeds were positioned in imbibed
424 filter paper, in sterile Petri dishes, and wrapped in aluminium foil. After 3 days at 21°C, young
425 seedling were transferred to square plates (12 x 12 cm) containing growth medium (as described
426 in (Giovannetti et al., 2017)). Both media used in this study were based on Long-Ashton solution
427 (with two levels of phosphate concentration -20 or 750 µM, LP or HP, respectively- as in
428 Supplementary Table 1) with 0.8% MES buffer (Duchefa Biochemie, Haarlem, The
429 Netherlands), 0.8% agarose (to minimize phosphate contamination), and adjusted to pH 5.7 with
430 1M KOH. After adding the medium, plates were dried, closed, overnight in a sterile laminar flow
431 hood. Two accessions, with four replicates per each accession, were placed on each plate. Each
432 plate was replicated, with mirrored position of each accession to minimize any positional growth
433 effects. Plates were placed vertically, and plants grown under long-day conditions (21°C, 16 h
434 light/8 h dark cycle) with white light bulbs emitting 50 µmol/m^2/s. Every day the position of
435 plates was shuffled to avoid positional effects.
436

437 **Analysis of root growth and anion content**

438 Each day at the same time, for 9 days, plates were scanned with CCD flatbed scanners (EPSON
439 Perfection V600 Photo, Seiko Epson, Nagano, Japan), and the images were used to quantify root
440 parameters using Brat 2.0 (as described in Giovannetti et al., 2017). After 10 days, roots and
441 shoots from 4 plants of each accession were weighed and frozen. For anion measurements in the
442 initial screening, frozen plant material from 4 biological replicates was then homogenized in 1
443 mL of deionized water, and the anions -nitrate, phosphate and sulfate- were separated by the
444 Dionex ICS-1100 chromatography system on an Dionex IonPac AS22 RFIC 4x250 mm analytic
445 column (Thermo Scientific, Darmstadt, Germany) with 4.5 mM $NaCO_3$/1.4 mM $NaHCO_3$ as
446 running buffer. LORE1 Lotus mutants were ordered from Lotus Base (Mun et al., 2016) and
447 homozygous plants selected with specific primers (Supplementary table 9).
448

449 **Genome-wide association studies and overlap analysis**

450 GWA mapping was conducted on the mean and median trait values using a mixed model
451 algorithm (Kang et al., 2008), which has been shown to correct for population structure
452 confounding (Seren et al., 2012), and using the homozygous SNP data from the Lotus accessions
453 (Shah et al., 2018). SNPs with minor allele counts less than 10 were not taken into account. The
454 significance of SNP associations was determined around the 5% FDR threshold computed by the
455 Benjamini–Hochberg–Yekutieli method to correct for multiple testing (Benjamini and Yekutieli,
456 2001) and genes within a 10-kb genomic region spanning each SNP were considered, taking into
457 account that LD decays to 0.2 in Lotus (Shah et al., 2018).

458 **Inorganic phosphate concentration measurements**

Shoots and roots were collected, weighed and ground into powder in liquid nitrogen. The powder was incubated at 98°C in NanoPure water, for 1 hr, centrifuged for 20 minutes at maximum speed. Then 25 uL of a dilution 1:10 were used to determine inorganic phosphate concentrations using the molybdate phosphate assay (Sigma), following kit instructions, as previously described (Ames, 1966). Each 96-well plate contained a calibration curve for assessing phosphate concentration.

Figures and statistical analysis

Data analysis and plots were conducted in Rstudio (RStudio Team, 2016) using the following packages: tidyverse, emmeans, UpSetR, corrplot, RColorBrewer, rmarkdown, multcompView and gplots. Plots were further modified for colours and layout in Adobe Illustrator CS6. All the scripts used to generate raw figures can be found (Supplementary file 1) and raw measurements data (Supplementary table 10). Number of replicates and statistical tests are indicated below every graph.

Acknowledgements

The authors thank Samantha Krasnodebski for her help in amplifying Lotus accessions, Anna Małolepszy for the initial common effort on Lotus projects, Santosh Satbhai and the members of the Busch lab for the training in the Brat system and GWAS, Ümit Seren for assistance on Lotus GWAPP website, Patrick Hüther and Niklas Schandry for their help with R, Yasin Dagdas for further supervision and hosting in the lab, Irene Klinkhammer and Bastian Welter for helping with the anions' quantification. Funding of this work was supported by the Austrian Academy of Science through the Gregor Mendel Institute, the Salk Institute for Biological Studies and a

Marie Skłodowska-Curie Individual Fellowship, number 749044 (to MG). Research in SK´s lab is supported by the Deutsche Forschungsgemeinschaft (DFG, German Research Foundation) under Germany´s Excellence Strategy – EXC-Nummer 2048/1.

References

Almario, J., Jeena, G., Wunder, J., Langen, G., Zuccaro, A., Coupland, G., and Bucher, M. (2017). Root-associated fungal microbiota of nonmycorrhizal Arabis alpina and its contribution to plant phosphorus nutrition. Proc. Natl. Acad. Sci. **114**: E9403–E9412.

Ames, B.N. (1966). [10] Assay of inorganic phosphate, total phosphate and phosphatases. In Methods in Enzymology, Complex Carbohydrates. (Academic Press), pp. 115–118.

Atwell, S. et al. (2010). Genome-wide association study of 107 phenotypes in a common set of Arabidopsis thaliana inbred lines. Nature **465**: 627–631.

Balzergue, C. et al. (2017). Low phosphate activates STOP1-ALMT1 to rapidly inhibit root cell elongation. Nat. Commun. **8**: 15300.

Baxter, I., Brazelton, J.N., Yu, D., Huang, Y.S., Lahner, B., Yakubova, E., Li, Y., Bergelson, J., Borevitz, J.O., Nordborg, M., Vitek, O., and Salt, D.E. (2010). A Coastal Cline in Sodium Accumulation in Arabidopsis thaliana Is Driven by Natural Variation of the Sodium Transporter AtHKT1;1. PLOS Genet. **6**: e1001193.

Benjamini, Y. and Yekutieli, D. (2001). The Control of the False Discovery Rate in Multiple Testing under Dependency. Ann. Stat. **29**: 1165–1188.

Bouain, N., Satbhai, S.B., Korte, A., Saenchai, C., Desbrosses, G., Berthomieu, P., Busch, W., and Rouached, H. (2018). Natural allelic variation of the AZI1 gene controls root growth under zinc-limiting condition. PLOS Genet. **14**: e1007304.

Briat, J.-F., Rouached, H., Tissot, N., Gaymard, F., and Dubos, C. (2015). Integration of P, S, Fe, and Zn nutrition signals in Arabidopsis thaliana: potential involvement of PHOSPHATE STARVATION RESPONSE 1 (PHR1). Front. Plant Sci. **6**.

Carbonnel, S. and Gutjahr, C. (2014). Control of arbuscular mycorrhiza development by nutrient signals. Front. Plant Sci. **5**.

Casale, F.P., Rakitsch, B., Lippert, C., and Stegle, O. (2015). Efficient set tests for the genetic analysis of correlated traits. Nat. Methods **12**: 755–758.

Castrillo, G., Teixeira, P.J.P.L., Paredes, S.H., Law, T.F., de Lorenzo, L., Feltcher, M.E., Finkel, O.M., Breakfield, N.W., Mieczkowski, P., Jones, C.D., Paz-Ares, J., and Dangl, J.L. (2017). Root microbiota drive direct integration of phosphate stress and immunity. Nature **543**: 513–518.

Cattaneo, P. and Hardtke, C.S. (2017). BIG BROTHER Uncouples Cell Proliferation from Elongation in the Arabidopsis Primary Root. Plant Cell Physiol. **58**: 1519–1527.

Chao, D.-Y., Baraniecka, P., Danku, J., Koprivova, A., Lahner, B., Luo, H., Yakubova, E., Dilkes, B., Kopriva, S., and Salt, D.E. (2014). Variation in sulfur and selenium accumulation is controlled by naturally occurring isoforms of the key sulfur assimilation enzyme ADENOSINE 5'-PHOSPHOSULFATE REDUCTASE2 across the Arabidopsis species range. Plant Physiol. **166**: 1593–1608.

Chen, W. et al. (2016). Comparative and parallel genome-wide association studies for metabolic and agronomic traits in cereals. Nat. Commun. **7**: 12767.

Chevalier, F., Pata, M., Nacry, P., Doumas, P., and Rossignol, M. (2003). Effects of phosphate availability on the root system architecture: large-scale analysis of the natural variation between Arabidopsis accessions. Plant Cell Environ. **26**: 1839–1850.

Choi, J., Summers, W., and Paszkowski, U. (2018). Mechanisms Underlying Establishment of Arbuscular Mycorrhizal Symbioses. Annu. Rev. Phytopathol. **56**: 135–160.

Di Laurenzio, L., Wysocka-Diller, J., Malamy, J.E., Pysh, L., Helariutta, Y., Freshour, G., Hahn, M.G., Feldmann, K.A., and Benfey, P.N. (1996). The SCARECROW gene regulates an asymmetric cell division that is essential for generating the radial organization of the Arabidopsis root. Cell **86**: 423–433.

Domergue, F., Vishwanath, S.J., Joubès, J., Ono, J., Lee, J.A., Bourdon, M., Alhattab, R., Lowe, C., Pascal, S., Lessire, R., and Rowland, O. (2010). Three Arabidopsis Fatty Acyl-Coenzyme A Reductases, FAR1, FAR4, and FAR5, Generate Primary Fatty Alcohols Associated with Suberin Deposition. Plant Physiol. **153**: 1539–1554.

Essigmann, B., Güler, S., Narang, R.A., Linke, D., and Benning, C. (1998). Phosphate availability affects the thylakoid lipid composition and the expression of SQD1, a gene required for sulfolipid biosynthesis in Arabidopsis thaliana. Proc. Natl. Acad. Sci. U. S. A. **95**: 1950–1955.

Gifford, M.L., Banta, J.A., Katari, M.S., Hulsmans, J., Chen, L., Ristova, D., Tranchina, D., Purugganan, M.D., Coruzzi, G.M., and Birnbaum, K.D. (2013). Plasticity Regulators Modulate Specific Root Traits in Discrete Nitrogen Environments. PLOS Genet. **9**: e1003760.

Giovannetti, M., Małolepszy, A., Göschl, C., and Busch, W. (2017). Large-Scale Phenotyping of Root Traits in the Model Legume Lotus japonicus. In Plant Genomics: Methods and Protocols, W. Busch, ed, Methods in Molecular Biology. (Springer New York: New York, NY), pp. 155–167.

Hammond, J.P., Broadley, M.R., White, P.J., King, G.J., Bowen, H.C., Hayden, R., Meacham, M.C., Mead, A., Overs, T., Spracklen, W.P., and Greenwood, D.J. (2009). Shoot yield drives phosphorus use efficiency in Brassica oleracea and correlates with root architecture traits. J. Exp. Bot. **60**: 1953–1968.

Hiruma, K., Gerlach, N., Sacristán, S., Nakano, R.T., Hacquard, S., Kracher, B., Neumann, U., Ramírez, D., Bucher, M., O'Connell, R.J., and Schulze-Lefert, P. (2016). Root Endophyte Colletotrichum tofieldiae Confers Plant Fitness Benefits that Are Phosphate Status Dependent. Cell **165**: 464–474.

Huang, X.-Y. et al. (2016). Nuclear Localised MORE SULPHUR ACCUMULATION1 Epigenetically Regulates Sulphur Homeostasis in Arabidopsis thaliana. PLOS Genet. **12**: e1006298.

Julkowska, M.M., Koevoets, I.T., Mol, S., Hoefsloot, H., Feron, R., Tester, M.A., Keurentjes, J.J.B., Korte, A., Haring, M.A., Boer, G.-J. de, and Testerink, C. (2017). Genetic Components of Root Architecture Remodeling in Response to Salt Stress. Plant Cell **29**: 3198–3213.

Kang, H.M., Zaitlen, N.A., Wade, C.M., Kirby, A., Heckerman, D., Daly, M.J., and Eskin, E. (2008). Efficient Control of Population Structure in Model Organism Association Mapping. Genetics **178**: 1709–1723.

Kellermeier, F., Armengaud, P., Seditas, T.J., Danku, J., Salt, D.E., and Amtmann, A. (2014). Analysis of the Root System Architecture of Arabidopsis Provides a Quantitative Readout of Crosstalk between Nutritional Signals. Plant Cell **26**: 1480–1496.

Kerdaffrec, E., Filiault, D.L., Korte, A., Sasaki, E., Nizhynska, V., Seren, Ü., and Nordborg, M. (2016). Multiple alleles at a single locus control seed dormancy in Swedish Arabidopsis. eLife **5**: e22502.

Kisko, M., Bouain, N., Safi, A., Medici, A., Akkers, R.C., Secco, D., Fouret, G., Krouk, G., Aarts, M.G., Busch, W., and Rouached, H. (2018). LPCAT1 controls phosphate

576 homeostasis in a zinc-dependent manner. eLife **7**: e32077.
577 **Koprivova, A., Giovannetti, M., Baraniecka, P., Lee, B.-R., Grondin, C., Loudet, O., and**
578 **Kopriva, S.** (2013). Natural Variation in the ATPS1 Isoform of ATP Sulfurylase
579 Contributes to the Control of Sulfate Levels in Arabidopsis. Plant Physiol. **163**: 1133–
580 1141.
581 **Lanfranco, L., Fiorilli, V., and Gutjahr, C.** (2018). Partner communication and role of nutrients
582 in the arbuscular mycorrhizal symbiosis. New Phytol. **220**: 1031–1046.
583 **López-Bucio, J., Hernández-Abreu, E., Sánchez-Calderón, L., Nieto-Jacobo, M.F.,**
584 **Simpson, J., and Herrera-Estrella, L.** (2002). Phosphate Availability Alters Architecture
585 and Causes Changes in Hormone Sensitivity in the Arabidopsis Root System. Plant
586 Physiol. **129**: 244–256.
587 **MacLean, A.M., Bravo, A., and Harrison, M.J.** (2017). Plant Signaling and Metabolic
588 Pathways Enabling Arbuscular Mycorrhizal Symbiosis. Plant Cell **29**: 2319–2335.
589 **Małolepszy, A. et al.** (2016). The LORE1 insertion mutant resource. Plant J. **88**: 306–317.
590 **Mora-Macías, J., Ojeda-Rivera, J.O., Gutiérrez-Alanís, D., Yong-Villalobos, L., Oropeza-**
591 **Aburto, A., Raya-González, J., Jiménez-Domínguez, G., Chávez-Calvillo, G., Rellán-**
592 **Álvarez, R., and Herrera-Estrella, L.** (2017). Malate-dependent Fe accumulation is a
593 critical checkpoint in the root developmental response to low phosphate. Proc. Natl.
594 Acad. Sci. **114**: E3563–E3572.
595 **Müller, J., Toev, T., Heisters, M., Teller, J., Moore, K.L., Hause, G., Dinesh, D.C.,**
596 **Bürstenbinder, K., and Abel, S.** (2015). Iron-Dependent Callose Deposition Adjusts
597 Root Meristem Maintenance to Phosphate Availability. Dev. Cell **33**: 216–230.
598 **Mun, T., Bachmann, A., Gupta, V., Stougaard, J., and Andersen, S.U.** (2016). *Lotus* Base:
599 An integrated information portal for the model legume *Lotus japonicus*. Sci. Rep. **6**:
600 39447.
601 **Oh, Y.J., Kim, H., Seo, S.H., Hwang, B.G., Chang, Y.S., Lee, J., Lee, D.W., Sohn, E.J., Lee,**
602 **S.J., Lee, Y., and Hwang, I.** (2016). Cytochrome b5 Reductase 1 Triggers Serial
603 Reactions that Lead to Iron Uptake in Plants. Mol. Plant **9**: 501–513.
604 **Okamoto, S., Shinohara, H., Mori, T., Matsubayashi, Y., and Kawaguchi, M.** (2013). Root-
605 derived CLE glycopeptides control nodulation by direct binding to HAR1 receptor kinase.
606 Nat. Commun. **4**: 2191.
607 **Orgiazzi, A., Ballabio, C., Panagos, P., Jones, A., and Fernández-Ugalde, O.** (2018).
608 LUCAS Soil, the largest expandable soil dataset for Europe: a review. Eur. J. Soil Sci.
609 **69**: 140–153.
610 **Paredes, S.H. et al.** (2018). Design of synthetic bacterial communities for predictable plant
611 phenotypes. PLOS Biol. **16**: e2003962.
612 **Puga, M.I. et al.** (2014). SPX1 is a phosphate-dependent inhibitor of PHOSPHATE
613 STARVATION RESPONSE 1 in Arabidopsis. Proc. Natl. Acad. Sci. **111**: 14947–14952.
614 **Ristova, D., Giovannetti, M., Metesch, K., and Busch, W.** (2018). Natural genetic variation
615 shapes root system responses to phytohormones in Arabidopsis. Plant J. **96**: 468–481.
616 **RStudio Team** (2016). RStudio: Integrated Development Environment for R (RStudio, Inc.:
617 Boston, MA).
618 **Sakuraba, Y., Kanno, S., Mabuchi, A., Monda, K., Iba, K., and Yanagisawa, S.** (2018). A
619 phytochrome-B-mediated regulatory mechanism of phosphorus acquisition. Nat. Plants
620 **4**: 1089.
621 **Satbhai, S.B., Setzer, C., Freynschlag, F., Slovak, R., Kerdaffrec, E., and Busch, W.** (2017).
622 Natural allelic variation of *FRO2* modulates *Arabidopsis* root growth under iron
623 deficiency. Nat. Commun. **8**: 15603.
624 **Secco, D., Wang, C., Shou, H., Schultz, M.D., Chiarenza, S., Nussaume, L., Ecker, J.R.,**
625 **Whelan, J., and Lister, R.** (2015). Stress induced gene expression drives transient DNA
626 methylation changes at adjacent repetitive elements. eLife **4**: e09343.

Seren, Ü., Vilhjálmsson, B.J., Horton, M.W., Meng, D., Forai, P., Huang, Y.S., Long, Q., Segura, V., and Nordborg, M. (2012). GWAPP: a web application for genome-wide association mapping in Arabidopsis. Plant Cell **24**: 4793–4805.

Shah, N. et al. (2018). Extreme genetic signatures of local adaptation during plant colonization. bioRxiv: 485789.

Slovak, R., Göschl, C., Su, X., Shimotani, K., Shiina, T., and Busch, W. (2014). A Scalable Open-Source Pipeline for Large-Scale Root Phenotyping of Arabidopsis. Plant Cell **26**: 2390–2403.

Stetter, M.G., Schmid, K., and Ludewig, U. (2015). Uncovering Genes and Ploidy Involved in the High Diversity in Root Hair Density, Length and Response to Local Scarce Phosphate in Arabidopsis thaliana. PLOS ONE **10**: e0120604.

Svistoonoff, S., Creff, A., Reymond, M., Sigoillot-Claude, C., Ricaud, L., Blanchet, A., Nussaume, L., and Desnos, T. (2007). Root tip contact with low-phosphate media reprograms plant root architecture. Nat. Genet. **39**: 792–796.

Tabata, R., Sumida, K., Yoshii, T., Ohyama, K., Shinohara, H., and Matsubayashi, Y. (2014). Perception of root-derived peptides by shoot LRR-RKs mediates systemic N-demand signaling. Science **346**: 343–346.

Turley, P. et al. (2018). Multi-trait analysis of genome-wide association summary statistics using MTAG. Nat. Genet. **50**: 229.

Volpe, V., Giovannetti, M., Sun, X.-G., Fiorilli, V., and Bonfante, P. (2016). The phosphate transporters LjPT4 and MtPT4 mediate early root responses to phosphate status in non mycorrhizal roots. Plant Cell Environ. **39**: 660–671.

Wang, X., Wang, Z., Zheng, Z., Dong, J., Song, L., Sui, L., Nussaume, L., Desnos, T.M., and Liu, D. (2019). Genetic dissection of Fe-dependent signaling in root developmental responses to phosphate deficiency. Plant Physiol.: pp.00907.2018.

Yang, S.-Y. et al. (2012). Nonredundant regulation of rice arbuscular mycorrhizal symbiosis by two members of the phosphate transporter1 gene family. Plant Cell **24**: 4236–4251.

Yu, J., Pressoir, G., Briggs, W.H., Vroh Bi, I., Yamasaki, M., Doebley, J.F., McMullen, M.D., Gaut, B.S., Nielsen, D.M., Holland, J.B., Kresovich, S., and Buckler, E.S. (2006). A unified mixed-model method for association mapping that accounts for multiple levels of relatedness. Nat. Genet. **38**: 203–208.

Supporting data

Supplementary Figure 1. Sulfate and nitrate concentration is not dependent on plant size

Supplementary Figure 2. Lotus japonicus natural variation of root responses to phosphate media levels over time

Supplementary Figure 3. Lotus japonicus primary root length is negatively correlated with root phosphate concentration in plants grown under phosphate limitation

Supplementary Figure 4. Number of hits (p-value < FDR) per trait in anions vs. Brat analysis

Supplementary Figure 5. Cytochrome B5 reductase and LRR mutants accumulate more phosphate than wt in high phosphate media

Supplementary Figure 6. Plant phosphate concentration is negatively correlated with plant

669 biomass when phosphate is a the limiting factor

670 Supplementary Figure 7. Cytochrome B5 reductase and LAMP mutants are not affected in root
671 growth over different phosphate concentration

672 Supplementary Figure 8. Manhattan plots leading to the identification of cytochrome B5
673 reductase locus

674 Supplementary Figure 9. Manhattan plots leading to the identification of LAMP

675 Supplementary Figure 10. LIMIX model of GWAS leading to the identification of LAMP locus

676 Supplementary Figure 11. LIMIX model of GWAS leading to the identification of cytochrome
677 B5 reductase

678 Supplementary Table 1. Modified Long-Ashton media solution

679 Supplementary Table 2. GWAS hit from LP:HP ratio of Lotus Brat results

680 Supplementary Table 3. GWAS hit from Lotus roots grown on LP media

681 Supplementary Table 4. GWAS hit from Lotus roots grown on HP media

682 Supplementary Table 5. GWAS hit from Lotus anion content

683 Supplementary Table 6. List of Lotus japonicus accessions

684 Supplementary Table 7. Statistics summary for cytochrome B5 reductase and LAMP mutants

685 Supplementary Table 8. Top 500 SNPs from anion and root traits with p-value < 10E-5

686 Supplementary Table 9. Primers and mutant plants used in this study

687 Supplementary Table 10. Raw data from root system analysis and anion measurements

688 Supplementary Table 11. GO enrichment for GWAS hits of root system traits from LP media

689 Supplementary Table 12. GO enrichment for GWAS hits of root system traits from HP media

690 Supplementary Table 13. List of significant SNPs above benjamini-Hochberg FDR threshold

691 Supplementary file 1. List of R codes and plots used in this study (Rmd file).

692

693

694

695

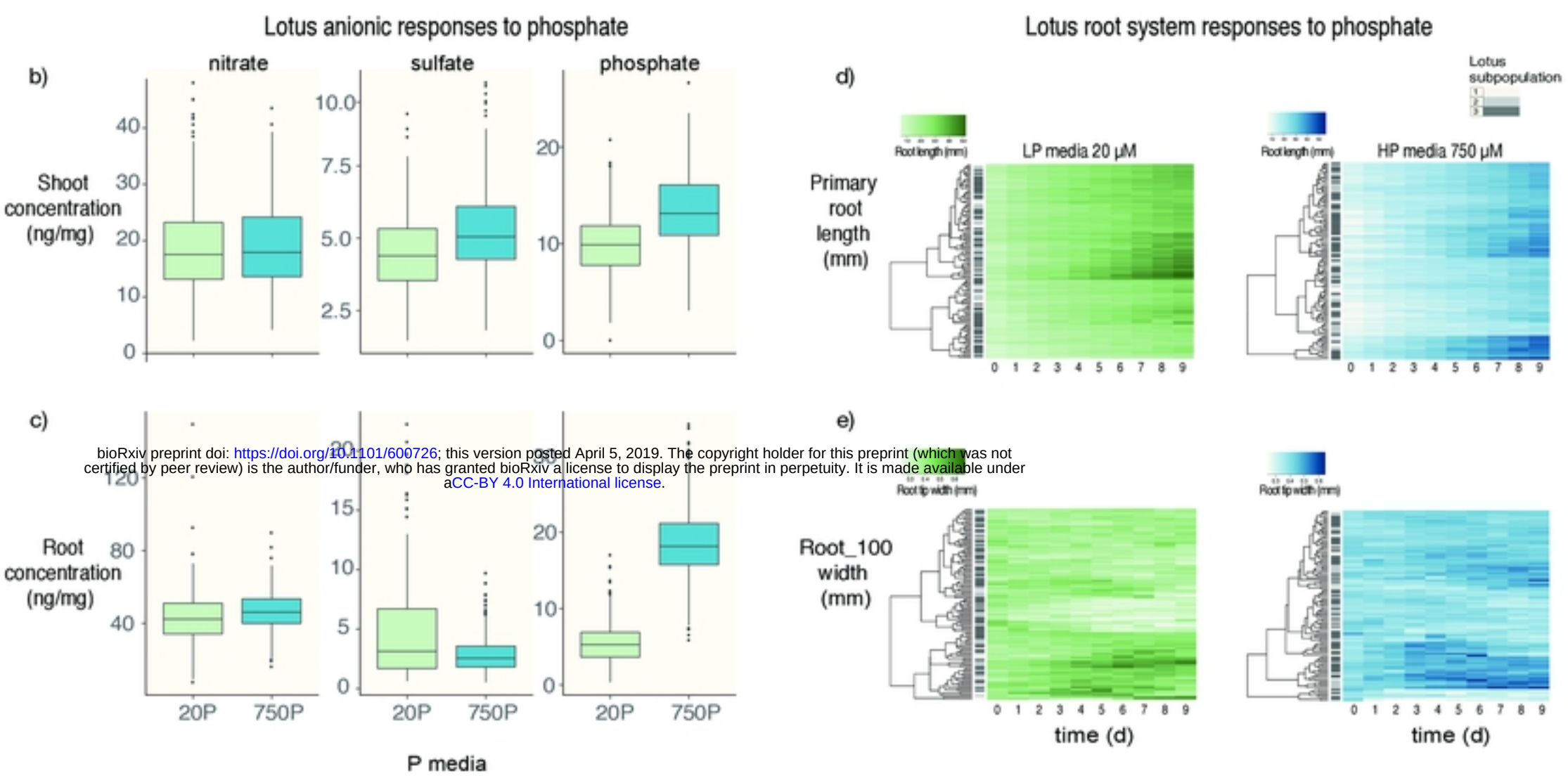

Fig. 1 Lotus japonicus natural variation of root responses to phosphate media levels over time. a) Set up of the experiment. One-hundred and thirty Lotus accessions were grown on low (20 µM) or high (750 µM) phosphate media for 9 days. Plates were scanned every day, and root traits were quantified and segmented using Brat. After 9 days, shoots and roots were harvested and nitrate, phosphate and sulfate concentration were measured. All the traits were then used for running GWAS. Here, we show representative traits of anions' accumulation and primary root traits of the Lotus panel. b-c) Concentration of anions in roots and shoots depends on the phosphate concentration in the media. Both shoot and root accumulation of anions' shows a significant effect of phosphate concentration in the media. A strong effect is shown by phosphate content in roots and shoots and sulfate content in shoots. d-e) Over a 9-day time course, Lotus natural accessions show a high diversity in root growth over LP and HP, both for primary root length and root width. Clustering of responses to nutrient is not dependent on Lotus subpopulation origin.

Figure 1

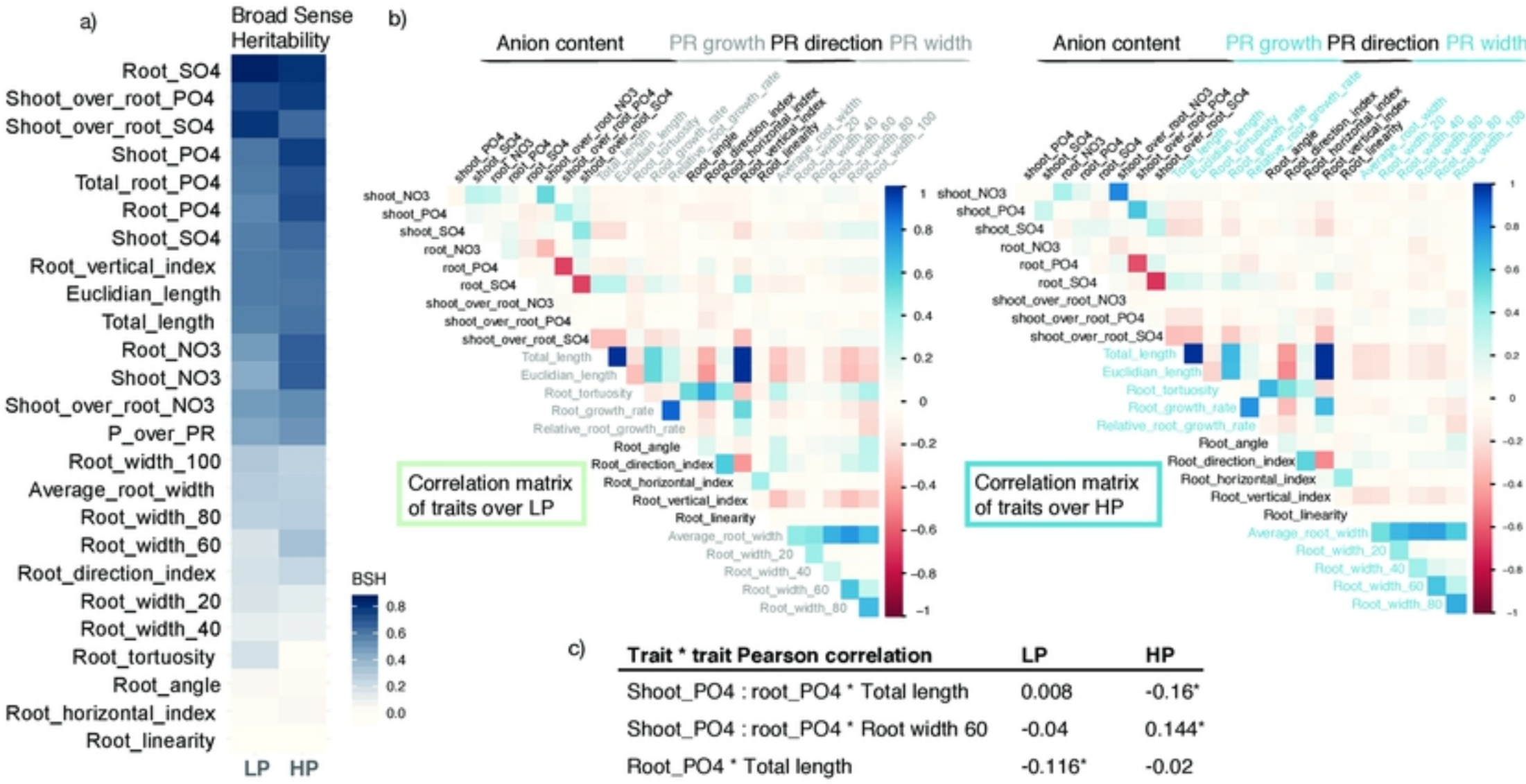

Fig. 2 Pattern of Lotus correlation among root and anions' traits and broad sense heritability at day 9 under LP or HP

a) Broad Sense Heritability of all measured traits on low and high phosphate. Highest heritability is shown by traits related to nutrient accumulation. Among root system architecture traits, those related to primary root length show higher broad sense heritability. b) Heatmap of Pearson's pairwise correlations on every measured trait (root system architecture and nutrient accumulation) on day 9. On a population level, the traits acquired by Brat show distinct and recursive features: root width from the different root parts are all positively correlated. A similar pattern is shown also by traits related to primary root growth, such as total length, Euclidian length, root vertical index. By contrast root width and length parameters are negatively correlated: the longer the root, the finer it gets. Correlation between root system architecture traits and tissue anions' concentration show the same pattern in LP and HP with a few exceptions. c) Total length and shootPO4:rootPO4 (phosphate translocation) do show an opposite behavior among the two conditions. In particular in low phosphate plates, primary root length is negatively correlated with root phosphate concentration in discordance with normal phosphate condition. By contrast, shootPO4:rootPO4 has a clear opposite pattern. Pearson's r value are indicated and the asterisk represents p value 0.05

Figure 2

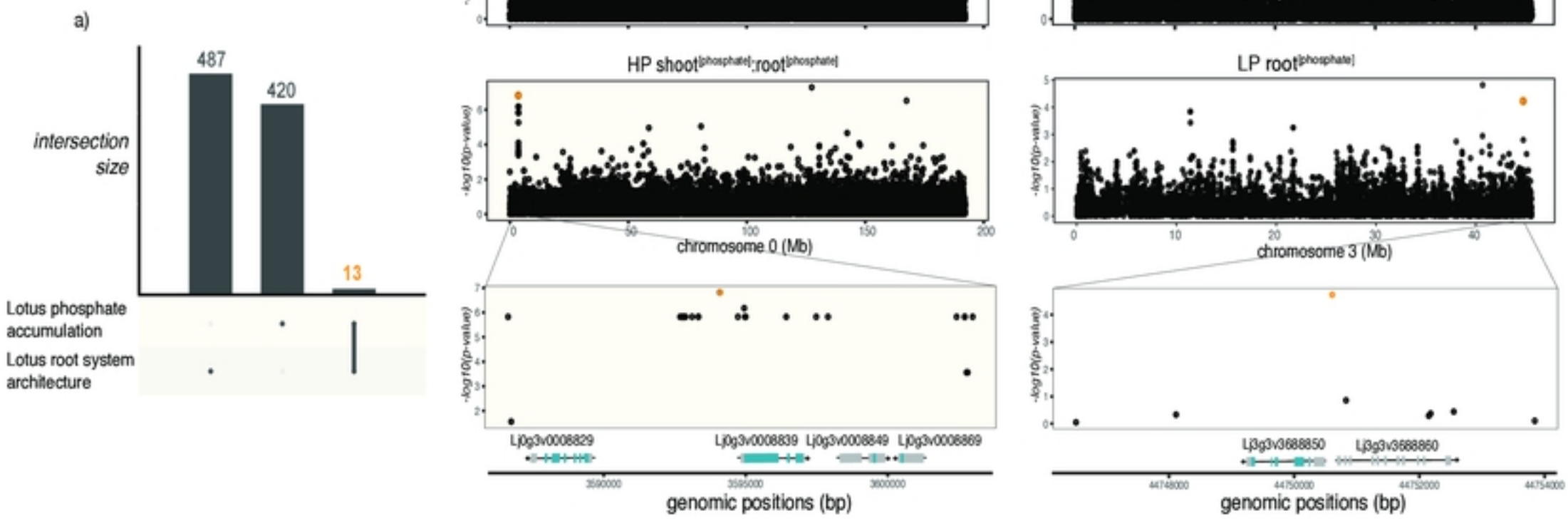

Fig. 3 Overlap between GWAS hits from root system architecture and phosphate accumulation

a) The intersection of candidate genes associated with changes in root system architecture (487) and phosphate accumulation traits (420) is 13, corresponding to 7 genomic regions. B) Manhattan plots of two traits leading to the identification of one genomic region on chromosome 0. A close-up on that region shows a 20kb region containing two protein-coding genes and two non-coding genes. c) Manhattan plots of the two traits leading to the identification of a genomic region on chromosome 3. A close-up on a 20kb region containing one single protein-coding genes, a cytochrome B5-reductase

Figure 3

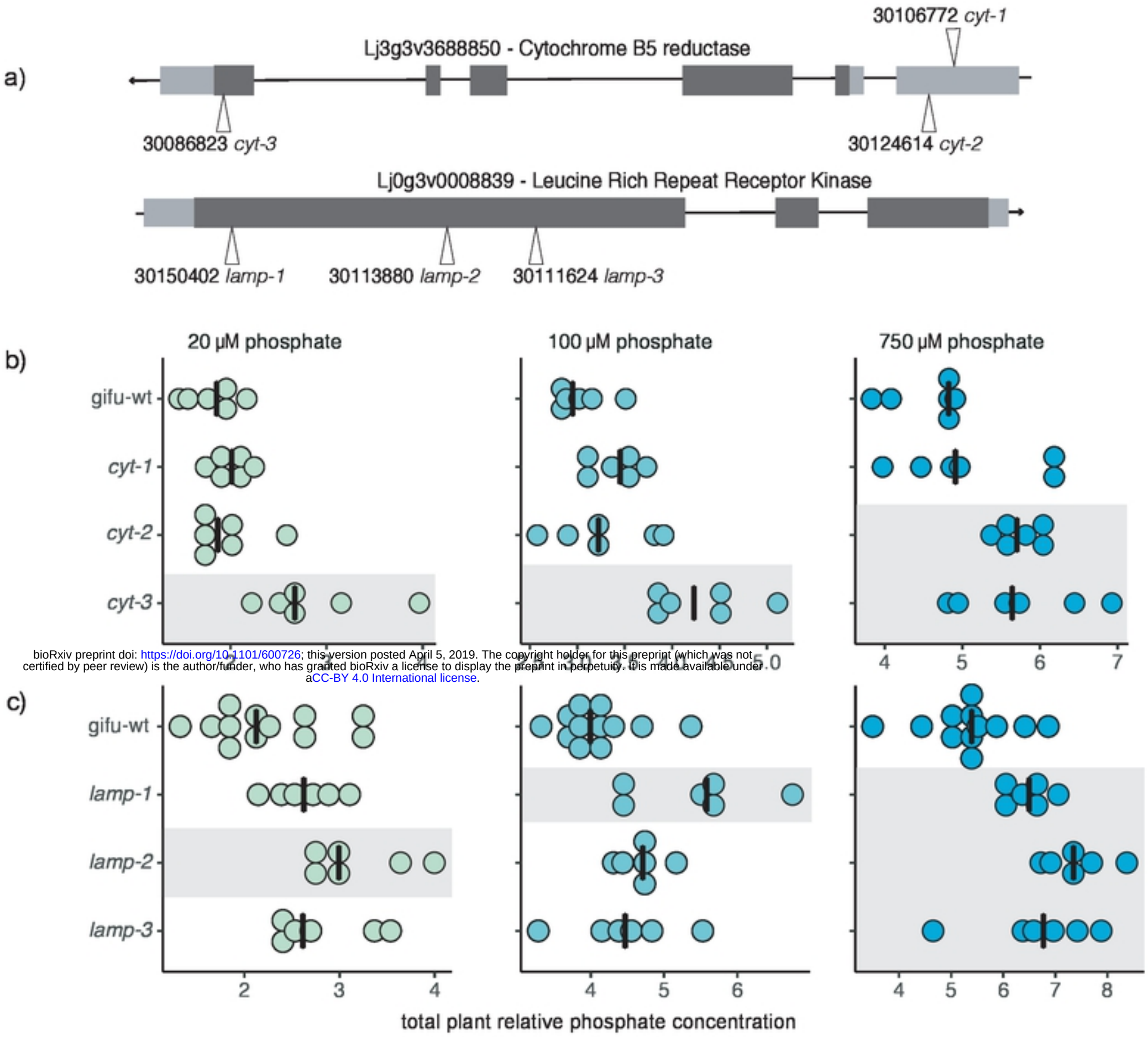

Fig. 4 Cytochrome B5 reductase and LRR mutants accumulate more phosphate than wt in high phosphate media

a) Gene structure and insertional mutants used in this study. Each number represents the Plant ID from Lotus Base. Three insertional mutants per each gene were used. b) Plant phosphate concentration levels of wt and LORE1 cytochrome B5 reductase insertional mutant plants growing under low (20 µM) or mid (100 µ M) or high phosphate level (750 µM). Whereas at low and mid concentration, only cyt3 show a significant difference compared to wt plants, at high phosphate concentration also cyt2 is accumulating significantly more phosphate. c) Total phosphate concentration of LRR-RK mutant plants and wt in the three phosphate media conditions. Both three LORE1 insertions show a higher phosphate accumulation compared to wt. Each dot represents a single plant and black vertical lines represent the median among the group. Levels of phosphate are expressed relative to wt root plants at 20 µM. Different shades represent different groups compared to wt, following Anova test on estimated marginal means (Tukey's adjusted p-value < 0.05).

Figure 4

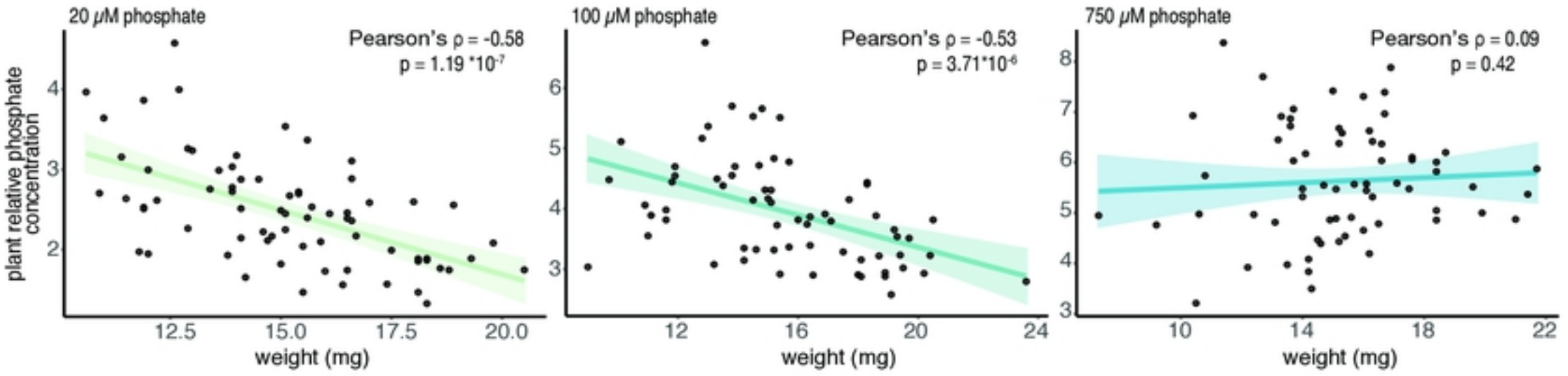

Fig. 5 Plant phosphate concentration is negatively correlated with plant biomass when phosphate is the limiting factor

Phosphate concentration levels of plants growing under low (20 μm) or mid (100 μM) phosphate is highly negatively correlated with plant biomass (Pearson's correlation is -0.58 and -0.53 respectively and p-value <10-6). By contrast under high phosphate level (750 μM), no significant correlation has been observed between plant biomass and plant phosphate concentration. Each dot represent a single plant from different experiments. Phosphate concentration is calculated relative to wt roots phosphate concentration under 20 μM. Colored lined and colored shades represents linear regression and 95% confidence intervals.

Figure 5